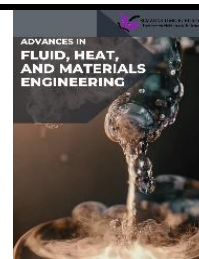




## Advances in Fluid, Heat and Materials Engineering

Journal homepage:  
<https://semarakilmu.com.my/journals/index.php/afhme/index>  
ISSN: XXXX-XXXX



# Effects of Different Biomass Feedstocks on Gasification Syngas Production Using Computational Fluid Dynamics

Nur Afiqa Syaheera Damahuri<sup>1</sup>, Ab Aziz Mohd Yusof<sup>2</sup>, Nurulnatisya Ahmad<sup>2</sup>, Ishkriyat Taib<sup>3</sup>, Kamariah Md Isa<sup>2,\*</sup>

<sup>1</sup> Faculty of Mechanical Engineering, UiTM Shah Alam, 40450, Shah Alam, Selangor, Malaysia

<sup>2</sup> College of Engineering (Mechanical), UiTM Johor Branch, Pasir Gudang Campus, 81750 Masai, Johor, Malaysia

<sup>3</sup> Faculty of Mechanical and Manufacturing Engineering, Universiti Tun Hussein Onn Malaysia, 86400 Parit Raja, Johor, Malaysia

### ARTICLE INFO

### ABSTRACT

#### Article history:

Received 30 August 2024

Received in revised form 5 September 2024

Accepted 18 September 2024

Available online 30 September 2024

#### Keywords:

Empty fruit bunch; rice husk; rice straw; biomass; gasification; computational fluid dynamics

The primary objective of this study was to assess whether biomass from empty fruit bunch (EFB), Rice Husk (RH), and Rice Straw (RS) can be effectively used for gasification. This study conducted a Computational Fluid Dynamics (CFD) simulation using ANSYS FLUENT and compare the results with published experimental data. First, Thermogravimetric and differential thermal analyses (TG-DTA) were performed to verify the usability of the feedstocks in gasification. The results show that EFB has a higher Carbon content and Higher Heating Value (HHV) than RH and RS, indicating a higher gasification potential. CFD simulations supported these findings, showing that EFB outperforms RH and RS in gasification potential by approximately 40% and 35%, respectively. The results demonstrated that EFB, with its higher efficiency, can offer significant environmental benefits compared to RH and RS.

## 1. Introduction

Coal reserves are depleting rapidly due to increased production, creating an urgent need for solutions. Biomass has emerged as a viable and sustainable alternative energy source [1]. The energy potential of biomass feedstock has attracted significant attention because it promotes sustainable energy use, improves energy efficiency, supports environmental preservation, and enables cost-effective advancements [2]. Despite being considered neutral and environmentally friendly, biomass energy has some drawbacks, including high moisture and hydrogen (H) content, contamination from poor-quality sources, low energy density, low calorific value, and varying composition and characteristics [1].

Biomass is a highly desired renewable energy source, mainly because of its easy acquisition and transportation, making it distinct from many other renewable sources. Moreover, biomass can be transformed into biofuels, thus gaining credibility and playing a significant role as an alternative energy source that benefits the environment [3]. Biomass can be any fuel derived from plant matter,

\* Corresponding author.

E-mail address: kamariahisa@uitm.edu.my

<https://doi.org/10.37934/afhme.2.1.6069>

including crop residues, wood, cultivated plants, and animal byproducts. Like coal, biomass can be used for heating, such as in wood stoves, or for generating power in plants [4]. Biomass combustion, which involves burning organic materials such as wood or crop waste to generate heat or power, has applications ranging from domestic heating to large-scale energy production.

The gasification of biomass involves a chemical process in which biomass reacts with gasifying agents, such as air, oxygen, and water, at high temperatures within gasifiers. In this process, biomass is chemically transformed into gas within a gasifier. Various factors related to gasifier design and fuel characteristics play a critical role in determining the gas production efficiency. These factors include the type of gasifying agent, biomass properties, moisture content, particle size, temperature within the gasification zone, operating pressure, and equivalence ratio [5]. The size and type of gasifier can also be constrained by factors such as inventory levels, moisture content, and fuel availability.

Gasifiers can be optimised using two primary methods: experimental testing and computer-aided simulation. The experimental approach typically involves conducting laboratory-scale tests on gasifiers. This method is often complex, time-consuming, and costly, and the accuracy of the results is limited. As a result, many researchers prefer a software-based approach for gasification analysis. One of the most commonly used techniques for optimising gasifiers is CFD [6].

This research aimed to use a CFD simulation model to examine biomass gasification at a small laboratory scale. This will be accomplished using ANSYS FLUENT, a widely used software. The accuracy of the CFD simulation was ultimately validated by comparing it with experimental data, demonstrating its potential for accurately predicting biomass gasification.

## **2. Methodology**

### *2.1 Determination of Biomass Properties*

This study tested gasification in three biomass materials: empty fruit bundles (EFB), rice husks (RH), and rice straws. The gasification process involves exposing these biomass materials to high temperatures while carefully controlling the oxygen and steam supply. This triggers a chemical reaction that breaks down biomass components, producing gases like carbon monoxide (CO), hydrogen (H<sub>2</sub>), and carbon dioxide (CO<sub>2</sub>), among others. The results of these experiments offer valuable insights into the suitability of biomass for gasification and its potential as a renewable energy source or raw material for related industries.

#### *2.1.1 Sample preparation*

Before conducting a laboratory analysis, it is essential to homogenise and reduce the sample size are essential to ensure that the collected sample accurately represents the entire batch. The samples were prepared according to the American Society for Testing of Materials (ASTM) standards ASTM D2013-86.

#### *2.1.2 Thermogravimetric and Differential Thermal Analysis (TG-DTA)*

Thermogravimetric and differential thermal analyses (TG-DTA) using a flow rate of 20 ml/min were conducted on all samples using nitrogen gas [7, 8]. The temperature was increased from 30 °C to 700°C at a rate of 10°C/min. At the beginning of each test, the biomass sample was placed in a sample pan situated in the TGA's heating zone. The instrument used for these analyses was Mettler Toledo TGA DSC 1, which combines Thermogravimetric Analysis (TGA) and Differential Scanning Calorimetry (DSC) techniques.

### 2.1.3 CHNSO elemental analysis

CHNSO elemental analysis, also known as organic elemental analysis or elemental microanalysis, measures the amounts of carbon (C), hydrogen (H), nitrogen (N), sulphur (S), and oxygen (O) present in a sample. In this process, a small amount of biomass is placed into the device and subjected to a high oxygen concentration, resulting in combustion. The combustion byproducts are then collected and analysed by gas chromatography. The analysis was conducted using a CHNS/O Analyser at the Instrumentation Laboratory of the Faculty of Chemical Engineering at UiTM Shah Alam, specifically with a FLASH2000 CHNS/O Analyser (brand-model CHNS-O).

### 2.1.4 Proximate analysis: Calorific value analysis

The proximate biomass analysis classifies materials based on the weight reduction proportions of volatile matter, fixed carbon, ash, and moisture. The heating values of the three dried solid samples were determined using a bomb calorimeter. This technique, known as calorific value analysis, was performed in-house using a Bomb Calorimeter (Brand IKA, Model: C-5000). In the bomb calorimeter, a 1-g sample was placed in a crucible and ignited electrically, allowing it to combust in pure oxygen. The ignition produces heat, which is indicated by a measurable increase in temperature [9].

## 2.2 CFD Simulation

### 2.2.1 CFD model development and validation

Modelling in ANSYS Fluent involves a comprehensive series of steps for accurate CFD analysis. First, the gasifier design was outlined using Geometry Creation. Mesh Generation was then conducted to discretize the mesh into a computational mesh of smaller elements or cells. To ensure the reliability of the simulation results, a Grid Independence Test (GIT) was conducted. This test determines the optimal mesh resolution that minimises numerical errors without unnecessarily increasing computational costs by comparing key outputs, such as velocity profiles, pressure distributions, and temperature gradients, across different mesh sizes. Figure 1 shows the design of the gasifier model and mesh generated using the ANSYS Workbench. After the simulation was conducted, the results were compared with those published by Chew et. al., [10] for validation.

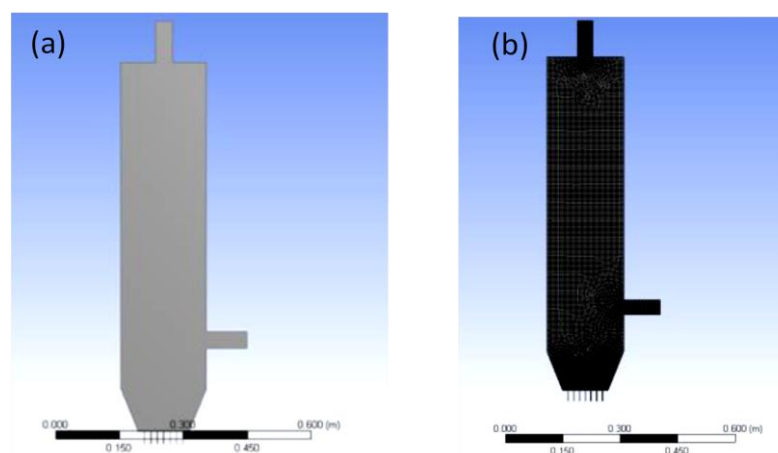


**Fig. 1.** Design of gasifier model (a) Gasifier design (b) Gasifier mesh

## 2.2.2 Gasification boundary conditions

Table 1 lists the boundary conditions of the gasifier design for all models. The inlet boundary was set as a mass flow rate about 10kg/h with 20% moisture, 80% dry matter of the biomass composition at 550°C of the temperature. The outlet was set as pressure at 1 bar with CO, CO<sub>2</sub>, H<sub>2</sub>, and CH<sub>4</sub> of gas composition. The wall temperature was set at 600°C with the heat flux was 50 kW/m<sup>2</sup>.

**Table 1**  
 Settings and boundary conditions

Properties	Value	References
Models	Multiphase Eulerian-Eulerian.	[11]
Multiphase models	Multi-fluid VOF model.	[12]
Viscous model	Realizable k-epsilon model.	[13]
Near wall treatment	Enhanced wall treatment.	[13]
Species model	Volumetric, species transport.	[13]
Turbulence-chemistry interaction	Finite-rate/eddy-dissipation .	[13]
Homogenous and Heterogenous reactions	Homogenous and heterogenous reactions were based the reactions shown by Kamariah <i>et al.</i> , [14] and Khan and Wang [15].	[14, 15]
Inlet Conditions	Mass flow rate	10 kg/h [16]
	Biomass composition	20% moisture, 80% dry matter [16]
	Temperature	550°C [17]
Outlet Conditions	Pressure	1 bar [17]
	Gas Composition	CO, CO <sub>2</sub> , H <sub>2</sub> , and CH <sub>4</sub> [17, 18]
	Wall Conditions	Wall temperature: 600°C [16]
	Heat flux	50 kW/m <sup>2</sup> [16]

## 3. Results

### 3.1 Proximate and Ultimate Analysis Results

Table 2 presents the results obtained from the final analysis, which are the proportions of carbon, hydrogen, nitrogen, and oxygen. The proximate analysis yields moisture levels, fixed carbon, ash, and volatile matter data. It is worth noting that all three biomass feedstocks had minimal amounts of sulphur, which can be attributed to their inherently low sulphur content. This shows that the tested biomass materials are environmentally favourable, as their extremely low sulphur content aligns with sustainability principles and aids in mitigating the potential environmental impacts of sulphur emissions. Higher heating value (HHV) is also calculated, measuring the energy content per unit mass.

The results of the proximate and ultimate analyses, together with the heating values, provide data on the composition and energy potential of the different fuel samples. Table 2 shows that RH and RS exhibit similar proximate compositions with moderate moisture content, substantial volatile matter content, and average heating values, suggesting comparable combustion characteristics. In contrast, EFB, characterised by low moisture content and high fixed carbon content, demonstrates superior energy density and efficiency, which is supported by its higher heating values. The ultimate analysis provides the elemental compositions of the samples, particularly nitrogen and carbon. These elements influence combustion behaviour and emissions profiles.

**Table 2**  
 Proximate and ultimate analysis of RH, RS, and EFB

	RH	RS	EFB
Moisture	8.7	8.5	6.3
Fixed Carbon	15.3	15.9	13.0
Ash	5.0	4.4	5.0
Volatile Matter	70.8	69.7	5.6
C	35.32	35.46	41.69
H	5.84	5.93	6.76
N	1.50	2.31	5.10
S	-	-	-
O	57.34	56.31	46.44
Higher Heating Value, HHV (MJ/kg)	10.04	10.39	15.46
Gross Calorific Value, GCV (kcal/kg)	3353	3222	3931

### 3.2 Simulation Results

#### 3.2.1 Velocity Distribution

Figures 2 to 4 show the range of biomass speeds for gas-phase (phase-1) and solid-phase (phase-2) reactions using all the chosen biomass materials. The simulation was performed to validate the accuracy of the gasification conditions within the gasifier. In addition, this simulation was carried out to understand the motions and reactions of the phases during the gasification process.

The contour plot (Figure 2 to Figure 4) illustrates the intermingling of phases within the gasifier during the gasification of empty fruit bunches (EFB), rice husks (RH), and rubber seeds (RS) at a time of 4.0 s. The velocity contours depict the speed of biomass movement, which was notably elevated near the biomass feedstock input, indicating the introduction of biomass into the gasifier. The gas phase contour illustrates the movement of gases from the lower section of the gasifier to its outlet.

The outcome demonstrates the successful completion of the two-phase simulation conducted on three selected biomasses. The gasification process's efficiency and performance are influenced by the velocity of the gas flowing through the gasifier. Increased velocities can facilitate the blending of gas with biomass, leading to enhanced conversion and improved reaction kinetics [19].

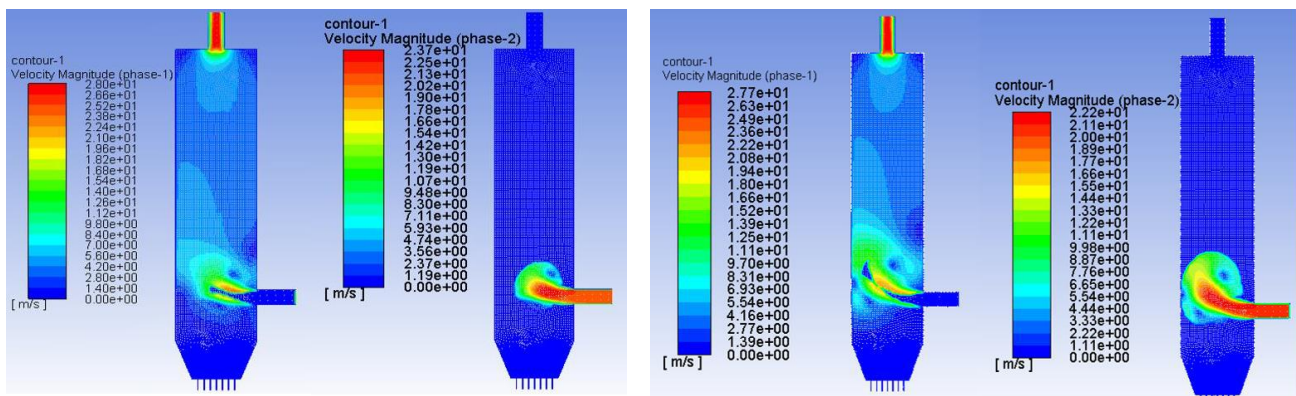


**Fig. 2.** Velocity magnitudes of RH phases 1 and 2 **Fig. 3.** Velocity magnitudes of RS phases 1 and 2

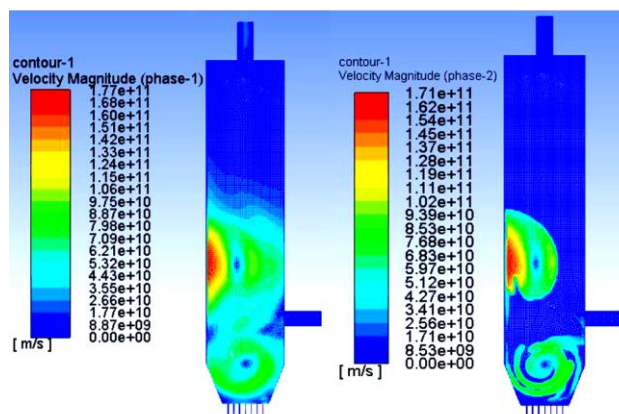


Fig. 4. Velocity magnitudes of EFB phases 1 and 2

### 3.2.2 Simulation model validation

Figure 5 represents the distribution of the mole fractions of the gas species CO, H<sub>2</sub>, and CH<sub>4</sub> across three sample biomass feedstocks within a gasifier: EFB, RS, and RH. In the EFB, methane (CH<sub>4</sub>) dominates with a mole fraction of 0.80, indicating a significant presence of methane relative to carbon monoxide (CO) and hydrogen (H<sub>2</sub>). RS shows a higher mole fraction of H<sub>2</sub> at 0.05 than EFB and RH, suggesting enhanced hydrogen production or retention under this condition. RH exhibits a more balanced distribution among CO (0.01), H<sub>2</sub> (0.03), and CH<sub>4</sub> (0.04), indicating a different operational setting where methane is present but less predominant than in EFB. These variations highlight how different conditions within the gasifier affect the composition of gas species, providing valuable insights into gasification processes and their efficiency in the production of desired gases such as H<sub>2</sub> and CH<sub>4</sub>.

Figure 5 highlights the validation of the simulation results by comparing them with experimental data obtained from existing literature. This procedure involved a meticulous analysis of the compositions of carbon monoxide (CO), hydrogen (H<sub>2</sub>), methane (CH<sub>4</sub>), and nitrogen (N<sub>2</sub>) in the outflow. These compositions were subsequently compared with the corresponding experimental results. The results indicate minimal disparities between the simulated and experimental values. This result demonstrates high precision and dependability in the simulation model because the gas compositions nearly match the measured concentrations. The comparison revealed that the simulation consistently forecasted greater mole fractions of CO and H<sub>2</sub> than the experimental findings.

In contrast, it predicted a slightly lower mole fraction of CH<sub>4</sub> than observed experimentally. The relative errors indicate the percentage deviation between the simulation and experimental results. Higher relative errors for CO and H<sub>2</sub> suggest that the simulation model overestimates these gases' concentrations under EFB conditions.

Conversely, the lower relative error for CH<sub>4</sub> indicates a closer agreement between the simulation and experimental data for methane. Table 3 shows that relative error values provide valuable insights into the performance and accuracy of the simulation model compared to experimental data in predicting the mole fractions of CO, H<sub>2</sub>, and CH<sub>4</sub> under EFB conditions. Further refinement of the simulation model or adjustments based on a detailed analysis of these discrepancies could enhance its predictive ability for gasification processes.

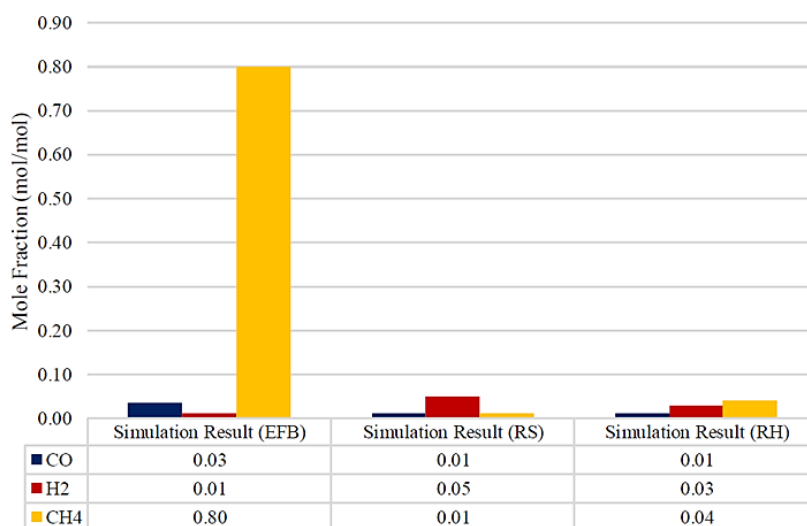


Fig. 5. Mole fraction distribution by species in the gasifier

Table 3

Relative errors in the validation results

Mole fraction	Experimental result EFB [12]	Simulation result (EFB)	Relative error
CO	0.05	0.03	24.44
H <sub>2</sub>	0.02	0.01	27.78
CH <sub>4</sub>	0.70	0.80	14.29

### 3.2.3 Syngas production and LHV results

During the gasification process, the biomass feedstock undergoes simultaneous pyrolysis and gasification. Pyrolysis, the more rapid of the two reactions, exerts a greater influence on syngas production when the volatile concentration is elevated. It is crucial to acknowledge that biomass samples containing higher amounts of volatile matter result in higher gas yields during pyrolysis, with carbon monoxide (CO) being the predominant gas component. Figure 6 shows the syngas compositions of the different biomass feedstocks: EFB, RH, and RS. Syngas composition is presented in molar percentages for three main components: CO, H<sub>2</sub>, and CH<sub>4</sub>. These gases are a key product of the gasification process and an essential intermediate for the generation of power and environmentally-friendly chemicals and fuels [20]. CH<sub>4</sub> is the dominant component of EFB syngas, which explains its higher energy content. This could be due to the inherent properties of the feedstock or the gasification process used. Carbon Monoxide (CO) and Hydrogen (H<sub>2</sub>) are present in smaller amounts than methane, but they are crucial in various chemical processes and syngas applications.

Based on Fig. 7, EFB has the highest LHV syngas production, indicating that it is the most efficient feedstock among the three. This is due to its higher methane content, CH<sub>4</sub>, which contributes significantly to the energy value of syngas. RH and RS have lower LHVs, with RH being slightly more efficient than RS. The data indicate that EFB is the most promising feedstock for syngas production in terms of energy efficiency. However, local availability and economic factors should also be considered when selecting feedstock for syngas production. Further research and optimisation of the gasification process can further increase the efficiency and applicability of biomass-derived syngas.

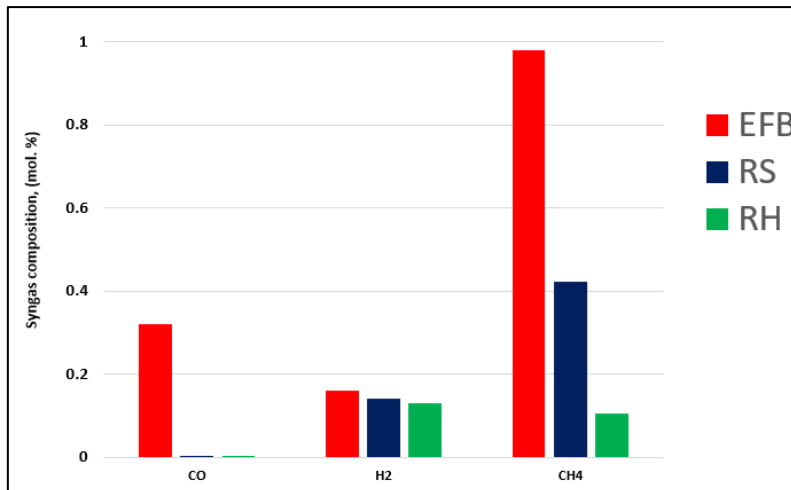


Fig. 6. Mole fraction distribution by species in the gasifier

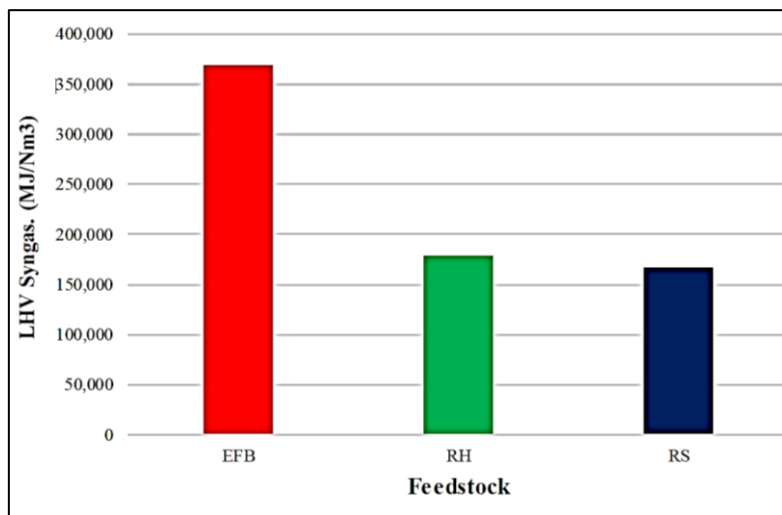


Fig. 7. Syngas production during RS gasification

#### 4. Conclusions

The obtained results offer significant insights into the gasification potential of biomass. A CFD simulation model for biomass gasification was successfully created and used to model the gasification process and predict the performance of different biomass feedstocks. The CFD simulation results were considered reliable, and the experimental data confirmed their accuracy. The validation demonstrated that the CFD model was accurate and reliable for predicting the gasification performance of biomass feedstock. The consistency between the simulated and actual data underscores the effectiveness of the CFD model as a tool for analysing and improving biomass gasification operations.

#### Acknowledgement

This research was funded by a grant from the Ministry of Higher Education of Malaysia (FRGS/1/2019/TK07/UITM/03/4).



## References

- [1] Jha, Gaurav, and S. Soren. "Study on applicability of biomass in iron ore sintering process." *Renewable and Sustainable Energy Reviews* 80 (2017): 399-407. <https://doi.org/10.1016/j.rser.2017.05.246>
- [2] Tirtea, Raluca-Nicoleta, Iustina Stanculescu, Gabriela Ionescu, Cora Bulmau, Cosmin Marculescu, and Dorin Boldor. "Transitory regime of wood biomass air gasification." In *2017 International Conference on Energy and Environment (CIEM)*, p. 390-393. IEEE, 2017. <https://doi.org/10.1109/CIEM.2017.8120799>
- [3] Ji-chao, Yang, and Behrooz Sobhani. "Integration of biomass gasification with a supercritical CO<sub>2</sub> and Kalina cycles in a combined heating and power system: a thermodynamic and exergoeconomic analysis." *Energy* 222 (2021): 119980. <https://doi.org/10.1016/j.energy.2021.119980>
- [4] Medlock, Kenneth B. "The economics of energy supply." In *International handbook on the economics of energy*. Edward Elgar Publishing, p. 848. 2009. <https://doi.org/10.4337/9781849801997.00008>
- [5] Pereira, Emanuele Graciosa, Jadir Nogueira Da Silva, Jofran L. De Oliveira, and Cássio S. Machado. "Sustainable energy: a review of gasification technologies." *Renewable and sustainable energy reviews* 16, no. 7 (2012): 4753-4762. <https://doi.org/10.1016/j.rser.2012.04.023>
- [6] Fernando, Niranjana, and Mahinsasa Narayana. "A comprehensive two dimensional computational fluid dynamics model for an updraft biomass gasifier." *Renewable Energy* 99 (2016): 698-710. <https://doi.org/10.1016/j.renene.2016.07.057>
- [7] Zou, Xun, Paulo Debiagi, Muhammad Ahsan Amjed, Ming Zhai, and Tiziano Faravelli. "Impact of high-temperature biomass pyrolysis on biochar formation and composition." *Journal of Analytical and Applied Pyrolysis* 179 (2024): 106463. <https://doi.org/10.1016/j.jaap.2024.106463>
- [8] Shukor, Hafiza, Hairul Nazirah Abdul Halim, Hui Lin Ong, Boon Beng Lee, and Mohd Hanif Mohd Pital. "Emerging technologies for future sustainability." <https://doi.org/10.1007/978-981-99-1695-5>
- [9] Babu, D., and R. Anand. "Influence of fuel injection timing and nozzle opening pressure on a CRDI-assisted diesel engine fueled with biodiesel-diesel-alcohol fuel." In *Advances in Eco-Fuels for a Sustainable Environment*, p. 353-390. Woodhead Publishing, 2019. <https://doi.org/10.1016/B978-0-08-102728-8.00013-9>
- [10] Chew, Jiuan Jing, Megan Soh, Jaka Sunarso, Siek-Ting Yong, Veena Doshi, and Sankar Bhattacharya. "Gasification of torrefied oil palm biomass in a fixed-bed reactor: Effects of gasifying agents on product characteristics." *Journal of the Energy Institute* 93, no. 2 (2020): 711-722. <https://doi.org/10.1016/j.joei.2019.05.010>
- [11] Shi, Shaoping, Christopher Guenther, and Stefano Orsino. "Numerical study of coal gasification using Eulerian-Eulerian multiphase model." In *ASME Power Conference*, vol. 42738, p. 497-505. 2007. <https://doi.org/10.1115/POWER2007-22144>
- [12] Khan, Jobaidur, and Ting Wang. "Implementation of a demoinsturation and devolatilization model in multi-phase simulation of a hybrid entrained-flow and fluidized bed mild gasifier." *International Journal of Clean Coal and Energy* 2, no. 3 (2013): 35-53. <http://dx.doi.org/10.4236/ijcce.2013.23005>
- [13] Md Isa, Kamariah, Kahar Osman, Nor Fadzilah Othman, Nik Rosli Abdullah, and Mohd Norhakem Hamid. "A multiphase eulerian-eulerian cfd simulation of fluidized bed gasification using malaysian low-rank coal-merit pila." *Key Engineering Materials* 740 (2017): 163-172. <https://doi.org/10.4028/www.scientific.net/KEM.740.163>
- [14] Isa, Kamariah Md, Kahar Osman, Nik Rosli Abdullah, Nor Fadzilah Othman, and Mohd Norhakem Hamid. "Gasifying agents type at lower temperature effect on bubbling fluidised bed gasification for low rank coal." *Progress in Computational Fluid Dynamics, an International Journal* 19, no. 1 (2019): 44-54. <https://doi.org/10.1504/PCFD.2019.097598>
- [15] Khan, Jobaidur, and Ting Wang. "Implementation of a demoinsturation and devolatilization model in multi-phase simulation of a hybrid entrained-flow and fluidized bed mild gasifier." *International Journal of Clean Coal and Energy* 2, no. 3 (2013): 35-53. <http://dx.doi.org/10.4236/ijcce.2013.23005>
- [16] Mishra, Somya, and Rajesh Kumar Upadhyay. "Review on biomass gasification: Gasifiers, gasifying mediums, and operational parameters." *Materials Science for Energy Technologies* 4 (2021): 329-340. <https://doi.org/10.1016/j.mset.2021.08.009>
- [17] Rabea, Karim, Stavros Michailos, Muhammad Akram, Kevin J. Hughes, Derek Ingham, and Mohamed Pourkashanian. "An improved kinetic modelling of woody biomass gasification in a downdraft reactor based on the pyrolysis gas evolution." *Energy Conversion and Management* 258 (2022): 115495. <https://doi.org/10.1016/j.enconman.2022.115495>
- [18] Yu, Jiahui, Shuai Wang, Kun Luo, Debo Li, and Jianren Fan. "Study of biomass gasification in an industrial-scale dual circulating fluidized bed (DCFB) using the Eulerian-Lagrangian method." *Particuology* 83 (2023): 156-168. <https://doi.org/10.1016/j.partic.2023.02.018>

- [19] Guo, Mengyao, Jiahui Yu, Shuai Wang, Kun Luo, and Jianren Fan. "Study of biomass gasification combined with CO<sub>2</sub> absorption in a dual fluidized bed (DFB) using the Eulerian-Lagrangian method." *Chemical Engineering Journal* 483 (2024): 148723. <https://doi.org/10.1016/j.cej.2024.148723>
- [20] AlNouss, Ahmed, Gordon McKay, and Tareq Al-Ansari. "Production of syngas via gasification using optimum blends of biomass." *Journal of Cleaner Production* 242 (2020): 118499. <https://doi.org/10.1016/j.jclepro.2019.118499>